Received: 23 April 2020 | Revised: 13 July 2020 | Accepted: 17 July 2020

DOI: 10.1111/cas.14588

ORIGINAL ARTICLE

Cancer Science WILEY

Bromo- and extraterminal domain protein inhibition improves immunotherapy efficacy in hepatocellular carcinoma

Chen Liu[1,2] | Xiaolong Miao[1,2] | Yao Wang[3] | Liang Wen[4] | Xiawei Cheng[5] | Deqiang Kong[1,2] | Pengwei Zhao[6] | Dandan Song[6] | Xinyi Wang[6] | Xianfeng Ding[3] | Hongguang Xia[7] | Weilin Wang[1,2] | Qiming Sun[6] | Weihua Gong[1,2]

[1]Department of Surgery, Second Affiliated Hospital of School of Medicine, Zhejiang University, Hangzhou, China

[2]Cancer Center, Zhejiang University, Hangzhou, China

[3]College of Life Sciences and Medicine, Zhejiang Sci-Tech University, Hangzhou, China

[4]Department of Hepatobiliary Surgery, First Affiliated Hospital of School of Medicine, Zhejiang University, Hangzhou, China

[5]Synthetic Biology and Biotechnology Laboratory, State Key Laboratory of Bioreactor Engineering, School of Pharmacy, East China University of Science and Technology, Shanghai, China

[6]Department of Biochemistry, and Department of Cardiology of Second Affiliated Hospital of School of Medicine, Zhejiang University, Hangzhou, China

[7]Department of Biochemistry and Molecular Biology of School of Medicine, Zhejiang University, Hangzhou, China

Correspondence
Weilin Wang and Weihua Gong, #88 Jie-Fang Road, Hangzhou, Zhejiang Province 310009, China.
Email: wam@zju.edu.cn (WW); weihuagong@zju.edu.cn (WG)

Qiming Sun, C-617 Research Building, #866 Yu-Hang-Tang Road, Hangzhou, Zhejiang Province 310058, China.
Email: qmsun@zju.edu.cn

Funding information
National Natural Science Foundation of China, Grant/Award Number: 81470527 and 81870306; Fundamental Research Funds for the Central Universities, Grant/Award Number: 2015XZZX004-21; Zhejiang Provincial 151 Talent Project, and Zhejiang Provincial Outstanding Youth Foundation, Grant/Award Number: LR13H020001; National Science Foundation for Outstanding Young Scholars of China, Grant/Award Number: 81522006

Abstract

Hepatocellular carcinoma (HCC) represents the majority of liver cancer and is the fourth most common cause of cancer-related death. Although advances in molecular targeted therapy have shown promise, none of these agents has yet demonstrated significant clinical benefit. Bromo- and extraterminal domain (BET) protein inhibitors have been considered potential therapeutic drugs for HCC but the biological activity remains unclear. This study found that BET protein inhibition did not effectively suppress the progression of HCC, using a transgenic HCC mouse model. Mechanistically, the BET protein inhibitor JQ1 upregulated the expression of programmed cell death-ligand 1 (PD-L1) on the plasma membrane in vivo and in vitro. Moreover, JQ1 enhanced the expression of Rab8A, which upregulated the expression of PD-L1 on the plasma membrane. This study also showed that JQ1 combined with anti-PD-L1 Ab effectively suppressed HCC progression, and this benefit was obtained by enhancing the activation and cytotoxic capabilities of CD8 T cells. These results revealed the crucial role and regulation of BET protein inhibition on the expression of PD-L1 in HCC. Thus, combining BET protein inhibition with immune checkpoint blockade offers an efficient therapeutic approach for HCC.

Abbreviations: BET, bromo- and extraterminal domain; DC, dendritic cell; HCC, hepatocellular carcinoma; HTVi, hydrodynamic tail vein injection; IFNγ, interferon-γ; IL-6, interleukin-6; LW/BW, liver weight / body weight; MDSC, myeloid-derived suppressor cell; MFI, mean fluorescent intensity; NK, natural killer; NPC, nonparenchymal cell; PD-1, programmed cell death-1; PD-L1, PD-1 ligand; SW/BW, spleen weight / body weight; TNF-α, tumor necrosis factor-α.

KEYWORDS
BET protein, hepatocellular carcinoma, immunotherapy, JQ1, PD-L1

1 | INTRODUCTION

Hepatocellular carcinoma is now the fourth leading cause of cancer-related deaths and the fifth most common cancer globally.[1,2] Due to its complications, heterogeneity, and lack of diagnostic biomarkers, the treatment of HCC is limited to surgical resection, liver transplantation, and local ablation at the early stage. Since sorafenib was approved as the first-line targeted small molecule drug for patients with advanced stage HCC in 2007, molecular targeted therapy for HCC has changed markedly.[3,4] In 2017, regorafenib was the first new FDA-approved second-line drug for the treatment of HCC. Subsequently, 2 PD-1 inhibitors, nivolumab and pembrolizumab, 2 tyrosine kinase inhibitors, lenvatinib and cabozantinib, as well as the mAb ramucirumab, have all received FDA approval.[5-7] However, none of these agents has yet demonstrated significant clinical benefit.

Inhibitors of BET proteins have been considered as potential therapeutic medicines for inflammatory diseases, cancer, metabolic disorders, and autoimmune diseases.[8,9] The BET proteins, including BRD2, BRD3, BRD4, and BRDT in mammals, share conserved bromodomains that bind to acetylated chromatin and function as transcriptional regulators.[10] Previous studies suggested that BET protein inhibitors could be considered as potential therapeutic drugs for liver cancer. BRD4 is overexpressed in HCC cells compared with that of normal hepatocytes. Knockdown of BRD4 inhibits the proliferation, migration, and invasion of HCC cell lines.[11,12] Treatment with the BET protein inhibitor JQ1 suppresses cell proliferation in HCC cell lines and the xenograft tumor model.[13] However, the therapeutic effects of BET protein inhibitors on primary liver cancer have rarely been reported.

The strategy of blocking inhibitory signaling pathways in T lymphocytes has remarkable influenced cancer therapy.[14,15] Blocking immune checkpoint protein inhibitors, such as PD-L1 and PD-1, have shown effectiveness against various solid tumors, including melanoma, non-small-cell lung cancer, and renal cancer.[16,17] Programmed cell death-ligand 1 is a membrane ligand that is upregulated on the cell surface of many types of cells in inflammation and/or in oncogenic lesions.[16] It binds with PD-1, a receptor on T cells, leading to Sh2p-driven dephosphorylation of the T cell receptor and its coreceptor CD28, suppressing antigen-driven activation of T cells.[18] Therapeutic Abs against the PD-L1/PD-1 axis can reactivate the antitumor immune response.[14] A series of clinical trials have evaluated a variety of combined therapy maneuvers of immune checkpoint inhibitors or with other drugs in advanced HCC; however, very limited therapeutic benefits have been observed so far.[19-21]

While evaluating the therapeutic effect of BET protein inhibition on HCC in vivo, we discovered that using JQ1 alone did not effectively suppress the HCC progression in a transgenic HCC mouse model. Mechanistically, BET protein inhibition upregulated the expression of PD-L1 on the surface of HCC cells by enhancing the expression of Rab8A. We tested a combination immunotherapy of JQ1 with anti-PD-L1 Ab, which effectively suppressed HCC progression in the HCC mouse model. These preclinical findings therefore suggest an efficient combination therapy strategy for HCC.

2 | MATERIALS AND METHODS

2.1 | Tumor model and treatments

Male C57BL6/J mice (6 weeks old) were purchased from Beijing Vital River Laboratory Animal Technology. All animal work was approved by the Institutional Animal Care and Use Committee of Zhejiang University. Animals were maintained in pathogen-free conditions and cared for according to the International Association for Assessment and Accreditation of Laboratory Animal Care policies and certification.

The transgenic HCC mouse model was established by HTVi. The plasmids (PT3-EF1a-C-Myc, PT/Caggs-NRas-V12, and pCMVSB11) were gifts from Dr Liang Wen at Zhejiang University. Nineteen micrograms of PT/Caggs-NRas-V12, 1 μg PT3-EF1a-C-Myc, and 2 μg pCMVSB11 were diluted in 2 mL 0.9% NaCl, sterile filtered, and injected into the lateral tail vein within 5-7 seconds.[22] Liver tumor nodules were visible at 4 weeks after HTVi.

For in vivo experiments, 5 doses of JQ1 (S7110; Selleck), which was dissolved in DMSO at a concentration of 50 mg/mL and subsequently diluted to a working concentration of 50 mg/kg in a solution of 10% hydroxypropyl β-cyclodextrin in sterile water (vehicle solution), or vehicle solution was i.p. injected over the course of 1 week. Anti-mouse PD-L1 Ab (BE0101; Bioxcell) was i.p. injected at a dose of 200 μg (or 200 μg rat IgG2b [BE0090; Bioxcell] as an isotype control) every other day for 3 doses as indicated.

2.2 | Cell line, culture conditions, treatment, viral infection, and transfection

Human HCC cell line (HepG2) was provided by Stem Cell Bank of the Chinese Academy of Sciences. HepG2 cells were maintained at 37°C with 5% CO_2 in DMEM (Gibco) supplemented with 10% heat-inactivated FBS (Gibco), penicillin, and streptomycin (15070063; Thermo Fisher).

For in vitro experiments, JQ1 was dissolved in DMSO at a concentration of 500 μmol/L and subsequently diluted to a working concentration of 500 nmol/L.

HepG2 Rab8A shRNA knockdown cells and HepG2 scrambled shRNA knockdown cells were obtained by

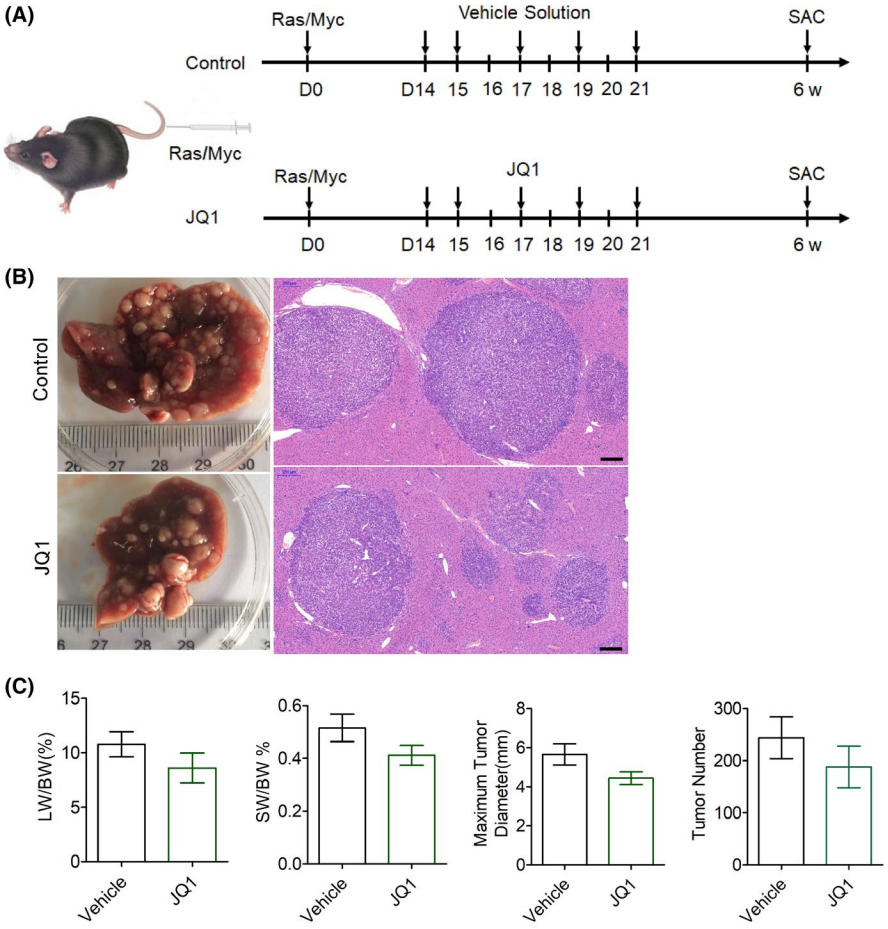

FIGURE 1 Inhibition of bromo- and extraterminal domain (BET) proteins cannot effectively suppress the progression of hepatocellular carcinoma in vivo. A, Schematic of the experimental procedure for JQ1 treatment. Mice were i.p. injected with JQ1 (50 mg/kg) at day (D) 14, 16, 18, 20, and 22 after plasmid transfection by hydrodynamic tail vein injection. All mice were killed (SAC) 6 wk after oncogene transfection for phenotypic analysis. B, Representative macroscopic views and H&E staining of liver sections of control and JQ1-treated mice. Magnification, ×50; scale bar, 200 μm. C, Tumor burdens were calculated by liver weight (LW) / body weight (BW) ratios, spleen weight (SW) / BW ratios, numbers of tumor nodules, or maximal diameters. Data are expressed as mean ± SEM (n = 6 per group) for any other groups versus the control group

lentivirus infection. The lentivirus contains shRNA to knockdown the expression of Rab8A. The sequence of Rab8A shRNA was 5′-CTCGATGGCAAGAGAATTAAA-3′. Lentivirus was produced following adenovirus packaging protocol.

For Rab8A or PD-L1 overexpression HepG2 cells, plasmids including Rab8a-Flag, Rab8A-GFP, the prenylation-deficient mutant Rab8A(C204Ser)-GFP, shRab8A-GFP, and PD-L1-mCherry were transfected into HepG2 cells by Lipofectamine 2000 (11668019; Thermo Fisher Scientific) according to the manufacturer's instructions. The exogenous Rab8A, PD-L1-mCherry, and Rab8A-GFP expression and the knockdown efficiency of endogenous Rab8A were confirmed by western blot assay (Figure S1).

2.3 | Statistical analysis

GraphPad Prism 7.0.4 software (GraphPad Software) was used for experimental data analysis. All experiments were independently repeated at least 3 times. The sample size was chosen according to well-established rules in the field. Statistical analyses were undertaken using Student's *t* tests. Values are expressed as the mean ± SEM. A *P* value of less than .05 was considered statistically significant.

Additional details of materials and methods are shown in Appendix S1 and Table S1.

3 | RESULTS

3.1 | Inhibition of BET proteins cannot effectively suppress progression of HCC in vivo

To investigate the treatment effect of BET protein inhibition on HCC cells in vitro, HepG2 cells were treated with DMSO or JQ1 (500 nmol/L) for 24 hours to test the cell function affected by JQ1. The CCK-8 proliferation assay showed that JQ1 significantly inhibited HepG2 cell proliferation ($P = .0085$) (Figure S2A). The cell cycle assay manifested that JQ1 treatment resulted in significantly decreasing the percentage of cells in the S ($P = .0041$) and G_2/M ($P = .0005$) phase and increasing in the percentage of cells in G_0/G_1 ($P = .0008$) phase (Figure S2B). Transwell assays revealed that JQ1 treatment significantly decreased cell migration ($P = .0062$) and invasion ($P = .0056$) compared with DMSO treatment in HepG2 cells (Figure S2C,D). These results indicated that JQ1 suppressed the proliferation, migration, and invasion of HCC cells in vitro, which is consistent with the results reported by previous studies.[11,12] Furthermore, to investigate the treatment effect of BET protein inhibition on HCC in vivo, we established a transgenic HCC mouse model. We delivered plasmids (*N-Ras/c-Myc*) with *sleeping beauty* transposase, which mediated genomic transgene integration to livers by HTVi. The drug administration strategy is shown in Figure 1A. Six weeks after HTVi, the mice were killed to analyze the parameters of tumor burden between the

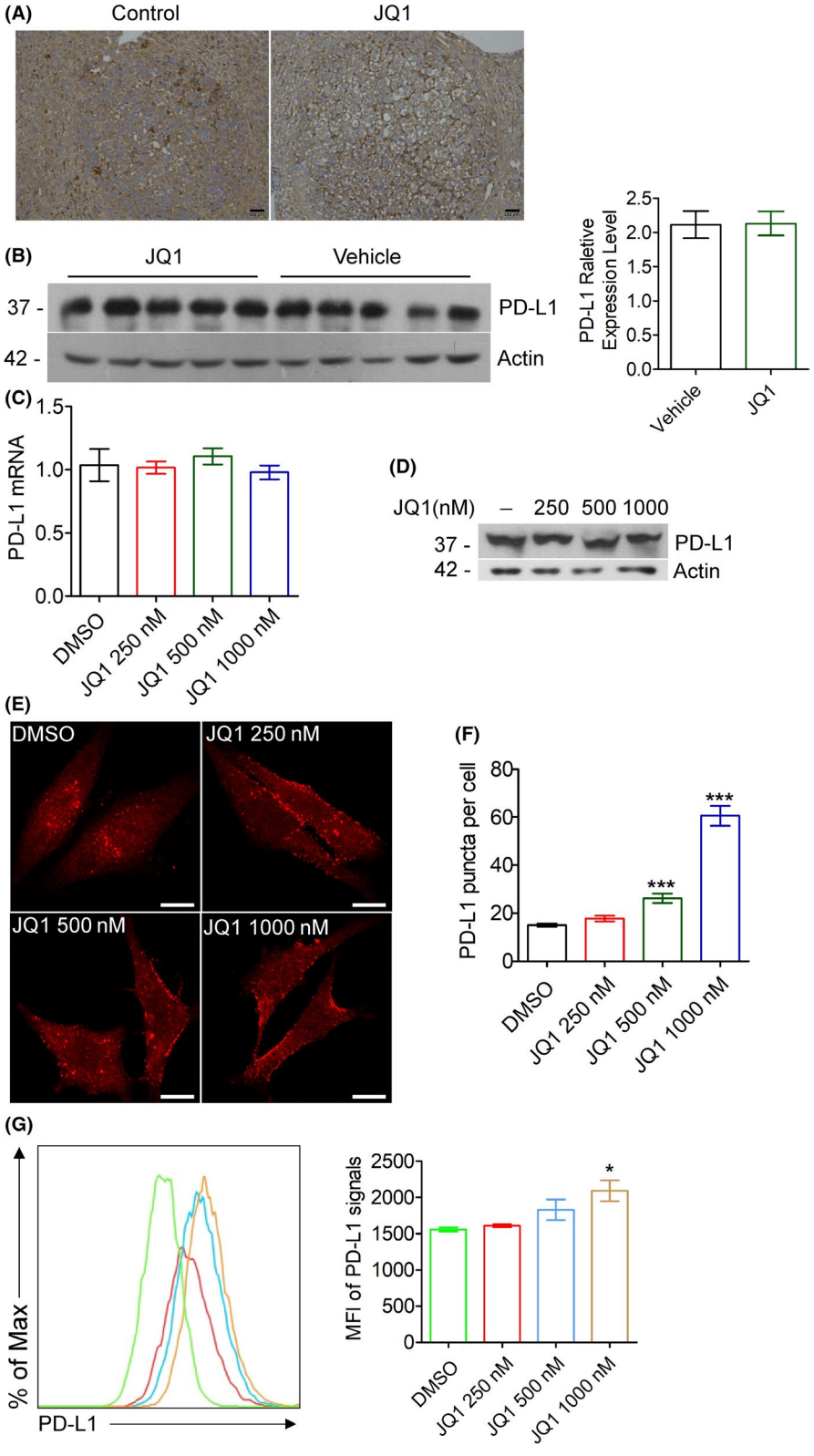

FIGURE 2 Inhibition of bromo- and extraterminal domain (BET) proteins upregulated the expression of programmed cell death-ligand 1 (PD-L1) on the plasmid membrane in vivo and in vitro. A, Representative immunostaining of PD-L1 in tumor areas in liver sections. Magnification, ×100; scale bar, 200 μm. B, Left panel: western blot analysis of PD-L1 protein levels in hepatocellular carcinoma tissues derived from JQ1 treatment group and control group mice, right panel: Relative expression level of PD-L1 in western blot. C, Fold change in *PD-L1* mRNA expression level in HepG2 cells treated with concentration gradients of JQ1 for 24 h. D, Western blot analysis of PD-L1 protein level in HepG2 cells treated with concentration gradients of JQ1 for 24 h. E, Immunofluorescence assay showing the expression of PD-L1 in HepG2 cells treated with concentration gradients of JQ1 for 24 h, fixed and analyzed by confocal microscopy and quantified in (F). At least 60 cells were counted for each group analysis. G, Flow cytometric analysis showing representative PD-L1 expression in HepG2 cells treated with concentration gradients of JQ1 for 24 h. Data are shown as mean ± SEM (*$P < .05$, ***$P < .001$). MFI, mean fluorescence intensity

JQ1 and control groups. We found that JQ1 treatment did not significantly suppress the progression of HCC compared to that of the control group by macroscopic examination and H&E staining of liver sections (Figure 1B). Additionally, there were no significant difference in the LW/BW ratio ($P = .2538$), SW/BW ratio ($P = .1370$), tumor number ($P = .3496$), or maximum tumor diameter ($P = .0807$) between the 2 groups (Figure 1C). However, the JQ1 treatment group showed a relatively attenuate trend in these parameters compared with the control group, especially for the parameter of maximum tumor diameter, showing a marginal difference between the 2 groups according to the *P* value. Taken together, these results indicate that BET protein inhibition suppresses the proliferation, migration, and invasion of HCC cells

in vitro, however, it cannot effectively inhibit HCC progression in the primary HCC mouse model.

3.2 | Inhibition of BET proteins upregulated expression of PD-L1 on plasma membrane in vivo and in vitro

As BET protein inhibition did not effectively suppress HCC progression in the transgenic HCC mouse model, it encouraged us to explore a more effective therapy strategy for HCC. We hypothesize that the unique immune microenvironment of the liver might play a vital role here. The strategy of blocking inhibitory signaling pathways in T lymphocytes, such as the PD-L1/ PD-1 axis, has been widely tested in various solid tumors.[23] Therefore, PD-L1 immunohistochemical staining of liver tissues was carried out. We found that PD-L1 was more concentrated around the plasma membrane in HCC lesions in the JQ1 treatment group than in the control group (Figure 2A). Western blot analysis was carried out on the tumor samples, and there was no significant difference in the total protein expression level of PD-L1 between the JQ1 treatment and control groups ($P = .9537$) (Figure 2B). In vitro, HepG2 cells were treated with JQ1 at concentrations of 250, 500, and 1000 nmol/L for 24 hours. No significant differences in the mRNA or protein expression levels of PD-L1 were observed as the concentration of JQ1 increased (Figure 2C,D). However, the immunofluorescence results revealed that as the concentration of JQ1 increased, the number of PD-L1 puncta in HepG2 cells increased and showed a significant difference when the concentration of JQ1 was 500 ($P = .0042$) or 1000 nmol/L ($P < .0001$) compared with that of DMSO treatment. The expression of PD-L1 on the plasma membrane was also significantly enhanced as the concentration of JQ1 increased (Figure 2E,F). Moreover, flow cytometry analysis showed that the MFI value of PD-L1 increased with increasing JQ1 concentration and showed a significant difference when the concentration of JQ1 was 1000 nmol/L compared with that of DMSO treatment ($P = .0211$) (Figure 2G). However, JQ1 treatment did not influence the PD-L2 expression on the plasma membrane of HCC cells (Figure S3A). Furthermore, we undertook a fractionation experiment, and the western blot analysis showed that the total PD-L1 level did not change with the concentration of JQ1 treatment increased in HepG2 cells; however, the level of PD-L1 on the plasma membrane increased and the level of PD-L1 in the cytosol decreased as the concentration of JQ1 treatment increased (Figure S3B). Together, these results show that BET protein inhibition upregulates the expression of PD-L1 on the plasma membrane in vivo and in vitro in HCC.

3.3 | Inhibition BET proteins enhances Rab8A expression, which upregulates PD-L1 expression on plasma membrane

As reported by previous studies, numerous members of Rab-GTPase family proteins, including Rab1, Rab3b, Rab5a, Rab5b, Rab6, Rab7, Rab8A, Rab9, Rab10, Rab11, Rab14, Rab25, Rab27a, and Rab39b,[24] participate in assisting transmembrane proteins to package into vesicles and transport among the plasma membrane and organelles.[25,26] We considered whether JQ1 could influence Rab-GTPase family protein expression, and then alter the PD-L1 expression on the plasma membrane. First, HepG2 cells were treated with DMSO or JQ1 (500 nmol/L) for 24 hours. The RT-PCR analysis revealed that the mRNA expression levels of *Rab8A* were significantly higher in the JQ1 treatment cells compared with that of the control cells, however, there were no significant differences in other Rab-GTPase family proteins between the 2 groups (Figure S4A). Western blot analysis showed that the protein expression level of Rab8A increased as the concentration of JQ1 increased in HepG2 cells (Figure 3A). Therefore, we hypothesized that JQ1 enhances the expression of Rab8A, which affects the expression of PD-L1 on the plasma membrane. Then, we constructed the HepG2 Rab8A-Flag cell line. Flow cytometry analysis showed that the MFI value of PD-L1 was significantly higher in HepG2 Rab8A-Flag cells than in HepG2 vector cells ($P = .0029$) (Figure 3B,C). We then constructed a HepG2 Rab8A shRNA knockdown cell line and undertook an immunofluorescence assay. The results suggested that JQ1 treatment significantly enhanced the expression of PD-L1 on the plasma membrane of HepG2 scrambled shRNA cells compared to that of DMSO treatment ($P = .0002$). However, this phenomenon did not occur in the HepG2 Rab8A shRNA knockdown cells ($P = .1380$). JQ1 treatment significantly increased the number of PD-L1 puncta in HepG2 scrambled shRNA knockdown cells compared to that of HepG2 Rab8A shRNA cells ($P < .0001$). Moreover, the number of PD-L1 puncta significantly decreased in the HepG2 Rab8A shRNA cells compared to that of HepG2 scrambled shRNA cells ($P = .0021$) (Figure 3D,E). To further confirm the direct link between Rab8A and PD-L1 translocation, we constructed the HepG2 PD-L1-mCherry and Rab8A-GFP cell line and HepG2 PD-L1-mCherry and shRab8A-GFP cell line. To exert the biological functions of Rab GTPase family proteins, they have to be membrane-bound, which is enabled by prenylation.[27] Therefore, we also used the HepG2 PD-L1-mCherry and Rab8A(C204Ser)-GFP cell line with prenylation-deficient mutant of Rab8A. Immunofluorescence assay results showed that the expression level of PD-L1 on the plasma membrane was significantly higher in HepG2 PD-L1-mCherry and Rab8A-GFP cells compared with the HepG2 PD-L1-mCherry and Rab8A(C204Ser)-GFP cells and HepG2 PD-L1-mCherry and shRab8A-GFP cells. Rab8A and PD-L1 colocalization on the plasma membrane was obvious in HepG2 PD-L1-mcherry and Rab8A-GFP cells (Figure S4B). Taken together, these results indicate that JQ1 treatment enhances the expression of Rab8A, which modulates the expression of PD-L1 on the plasma membrane.

3.4 | Inhibition of BET proteins combined with anti-PD-L1 Ab effectively suppresses progression of HCC

For an immunotherapy effect by blocking the PD-1/PD-L1 axis requires PD-L1 expression,[28] BET protein inhibition-induced PD-L1 expression on the plasma membrane prompted us to explore a new

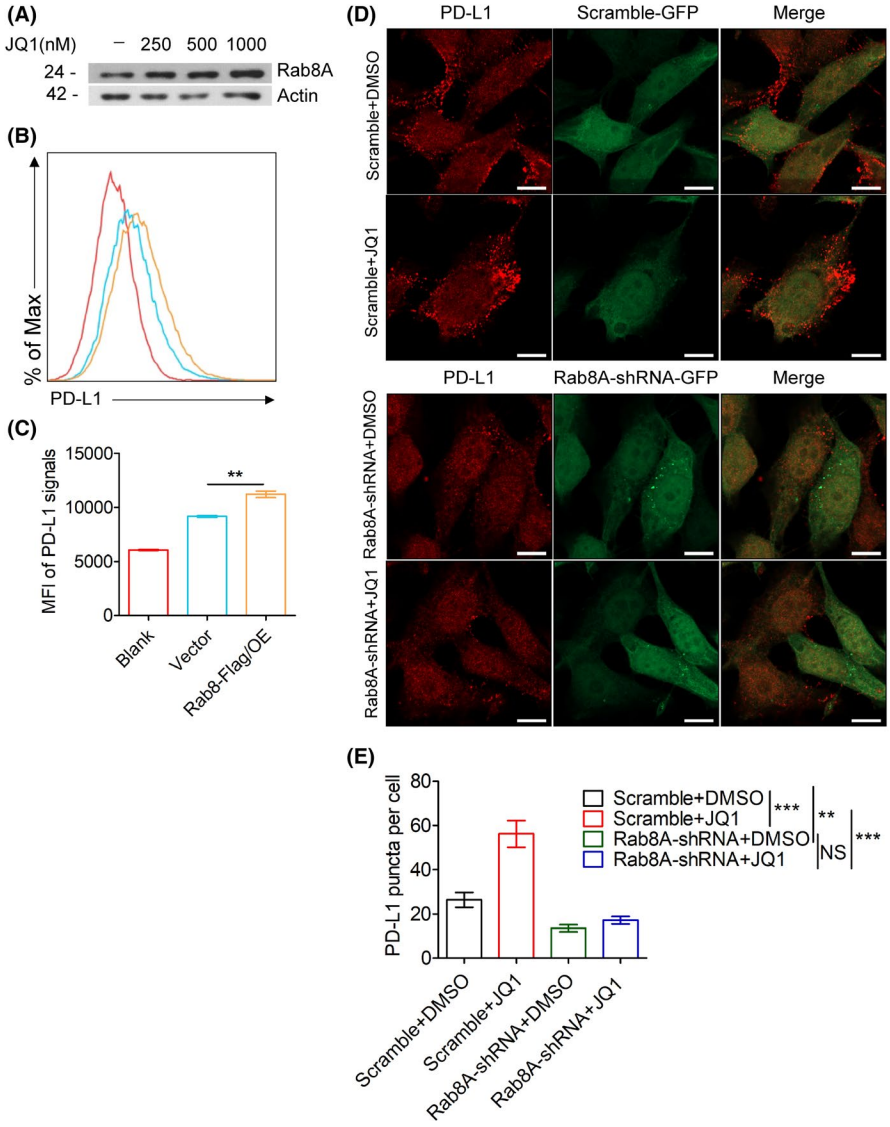

FIGURE 3 Inhibition of bromo- and extraterminal domain (BET) proteins enhances the expression of Rab8A, which upregulates the expression of programmed cell death-ligand 1 (PD-L1) on the plasma membrane. A, Western blot analysis of Rab8A protein levels in HepG2 cells treated with concentration gradients of JQ1 for 24 h. B, Flow cytometric analysis showing representative PD-L1 expression in HepG2 Rab8A-Flag cells and HepG2 vector cells. C, Quantification of the mean fluorescence intensity (MFI) of PD-L1 expression in HepG2 Rab8A-Flag cells compared with that of HepG2 vector cells. Blank, blank control. D, Immunofluorescence assay showing the effect of Rab8A on the expression of PD-L1. HepG2 Rab8A shRNA knockdown cells and HepG2 scrambled shRNA knockdown cells obtained by lentivirus infection were fixed, stained with PD-L1 Abs, and analyzed by confocal microscopy. Scale bar, 10 μm. E, Quantification of the number of PD-L1 puncta. At least 60 cells were counted for each group analysis. Data are shown as mean ± SEM (**$P < .01$, ***$P < .001$). NS, $P \geq .05$

therapeutic strategy for HCC by using a combined treatment of JQ1 with anti-PD-L1 Ab. The drug treatment strategy is shown in Figure 4A. The mice were killed for phenotypic analysis at 6 weeks after HTVi. We found that treatment with either JQ1 or anti-PD-L1 Ab failed to ameliorate the tumor burden, manifesting similar liver sizes, maximal tumor diameters, and numbers of tumor nodules as those of the control group. However, the combination of JQ1 and anti-PD-L1 Ab significantly ameliorated tumor progression compared with that of the control group, as measured by macroscopic analysis, H&E staining, LW/BW ratios ($P = .0412$), SW/BW ratio ($P = .0047$), maximal tumor diameters ($P = .0035$), and the number of tumor nodules ($P = .0034$) (Figures 4B-E and 5A). Moreover, we detected no significant differences in Ki67-positive cell ratios in the tumor areas in the anti-PD-L1 Ab group compared to those of the control group, and the JQ1 group showed a marginal difference compared to those of the control group ($P = .0741$); however, the combination of JQ1 and anti-PD-L1 Ab significantly suppressed the Ki67-positive cell ratios in the tumor areas compared to those of the control group ($P < .0001$) (Figure 5B). Mouse survival analysis showed median survival times of 73.0, 75.5, 84.0, and 95 days for the control, anti-PD-L1 Ab, JQ1, and combination groups, respectively. Overall, the survival time was similar between the anti-PD-L1 Ab and control groups. However, compared to the survival time of the control group, the JQ1 group showed significantly longer survival times. Moreover, the combination group showed the most significant increase in survival (Figure 5C). To evaluate the safety and toxicity of the drug treatment, mouse body weight was measured during the treatment process. The results showed that body weight was not significantly affected by the drug treatment among these 4 groups (Figure S5A). Taken together, these data show that combined treatment with BET protein inhibition and anti-PD-L1 Ab effectively suppresses the progression of HCC.

3.5 | Sensitization of PD-L1 blockade by inhibition of BET proteins boosts antitumor immunity in liver

We further explored the underlying mechanisms for the enhanced tumor-inhibitory effect of this combined therapeutic strategy.

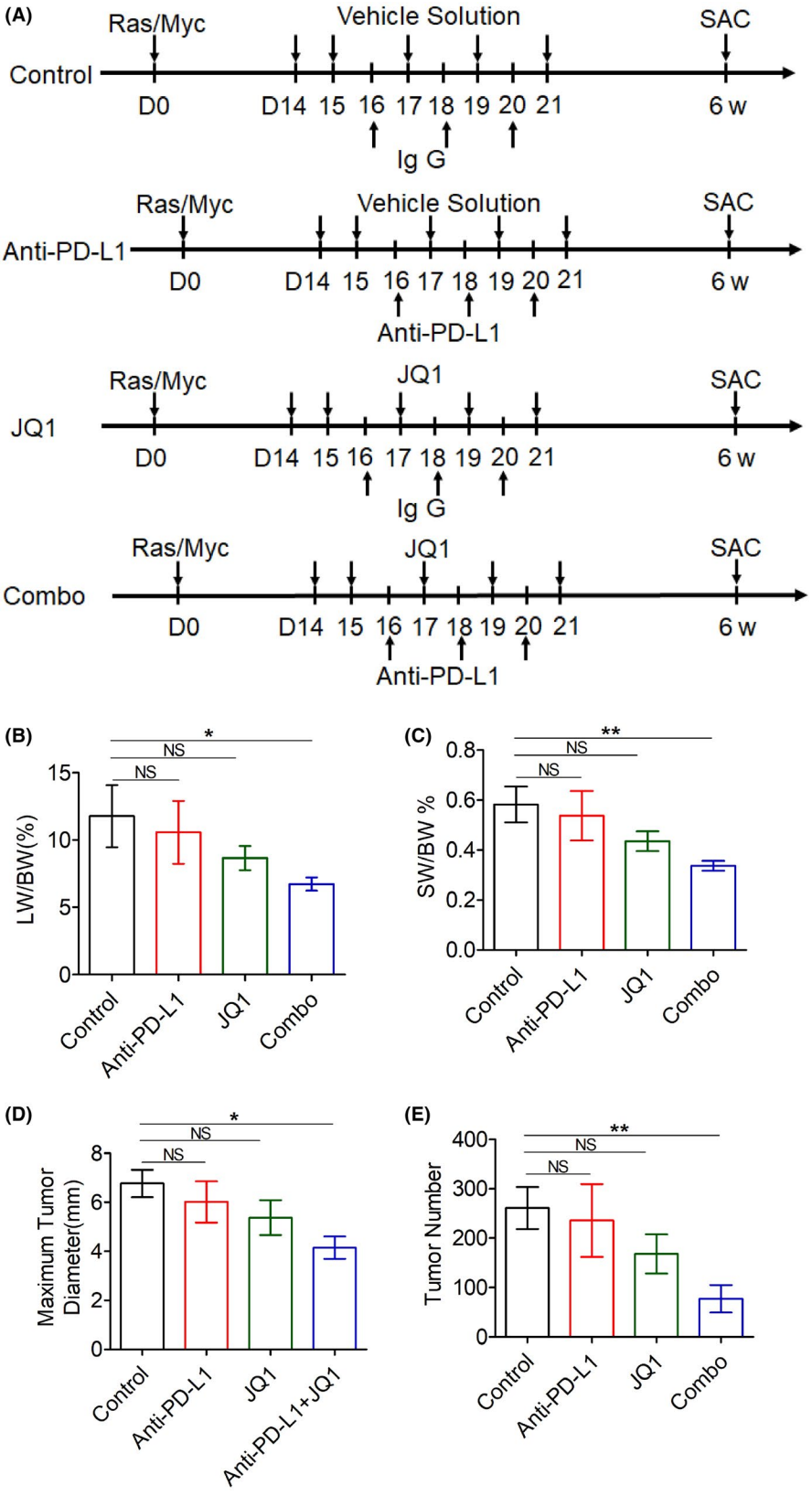

FIGURE 4 Inhibition of bromo- and extraterminal domain (BET) proteins combined with anti-programmed cell death-ligand 1 (PD-L1) Abs effectively suppressed the progression of hepatocellular carcinoma. A, Schematic of the experimental procedure for JQ1, anti-PD-L1 Ab, or the combination treatment. Plasmids were transfected into all mice at day 0. JQ1 (50 mg/kg) (or vehicle solution) was i.p. injected at days (D) 14, 16, 18, 20, and 22, and anti-PD-L1 Ab (or isotype IgG) was i.p. injected at days 17, 19, and 21. All mice were killed (SAC) 6 weeks after oncogene transfection for phenotypic analysis. B-E, Tumor loads were evaluated by liver weight (LW) / body weight (BW) ratios (B), spleen weight (SW) / BW ratios (C), maximal diameters (D), and the numbers of nodules (E). Data are shown as mean ± SEM (*$P < .05$, **$P < .01$). NS, $P \geq .05$

N-Ras/C-Myc-transfected mice received different therapeutic treatments, as shown in Figure 4A, and were killed 2 days after the last dose of JQ1 or vehicle solution. After in situ liver perfusion and isolation of NPCs, several innate and adaptive immune cell subsets of liver were analyzed. The ratios of each cell subset to the total number of NPCs were calculated. The innate immune cell subsets were analyzed by flow cytometry including NK cells ($CD4^-NK1.1^+$), macrophages ($CD11b^+F4/80^+$), MDSCs ($CD11b^+Gr1^+$), and DCs

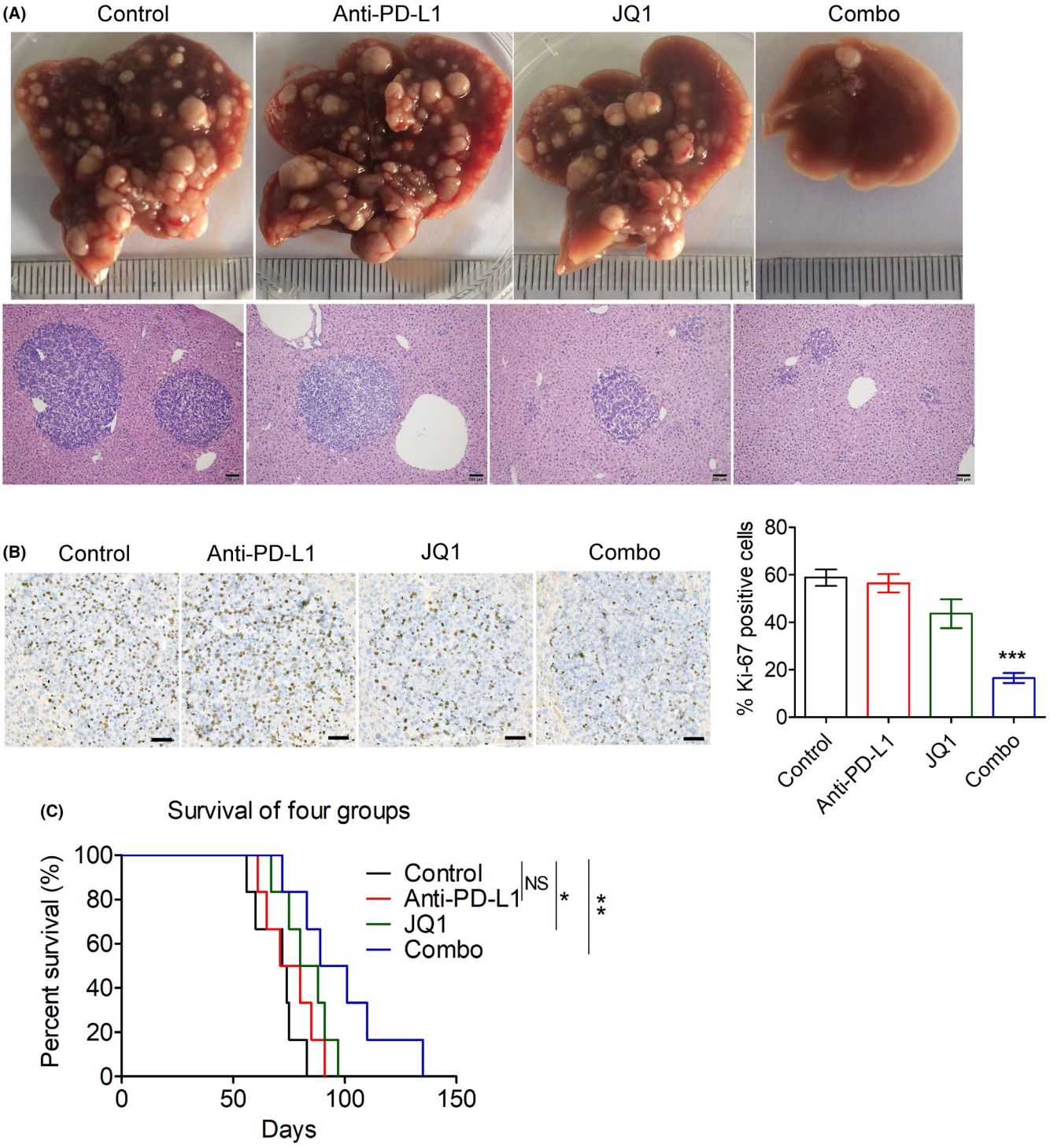

FIGURE 5 Inhibition of bromo- and extraterminal domain (BET) proteins combined with anti-programmed cell death-ligand 1 (PD-L1) Abs effectively suppressed the progression of hepatocellular carcinoma. A, Representative macroscopic views and H&E-stained liver sections in control, JQ1, anti-PD-L1 Ab, and combination treatment mice. Magnification, ×100; scale bar, 200 μm. B, Left panel: representative immunostaining of Ki67 in tumor areas. Magnification, ×200; scale bar, 200 μm. Right panel: quantification of $Ki67^+$ tumor cell numbers per field. C, Mouse Kaplan-Meier survival curve of the 4 treatment groups. When the mice were found to be feeble due to tumor burden, they were euthanized, and the date of death was recorded as the next day. Log-rank test, n = 6 per group. Data are shown as mean ± SEM (*$P < .05$, **$P < .01$, ***$P < .001$). NS, $P \geq .05$

(MHC II^+ $CD11c^+$). We found that there was no significant difference in the ratio of NK cells (Figure 6A,B), MDSCs (Figure 6C,D), DCs (Figure 6E,F), or macrophages (Figure 6G-I) among these groups. We also analyzed the adaptive immune cells, including conventional CD4 T cells ($CD4^+$) and cytotoxic CD8 T cells ($CD4^-CD8^+$). There was no significant difference in the ratio of CD4 T cells among these groups

(Figure 7A,B). Interestingly, the ratio of CD8 T cells was significantly increased in the combination group compared to that of the control group ($P = .0059$); however, treatment with either JQ1 or anti-PD-L1 Ab did not result in a significant difference in the ratio of CD8 T cells compared with the control group (Figure 7A,C). Furthermore, the activation ($CD44^+CD62L^-$) of CD8 T cells was analyzed, and JQ1 combined with anti-PD-L1 Ab further significantly boosted the activation of CD8 T cells compared with that of the control group ($P = .0018$) (Figure 7D,E). We also isolated CD8 T cells from NPCs and tested the mRNA levels of *granzyme B*, *perforin*, *TNF-α*, *IFN-γ*, and *IL-6*. JQ1 treatment significantly increased *IFN-γ* mRNA levels compared to those of the control ($P = .0018$), but anti-PD-L1 Ab treatment had no effect; the combination also significantly increased *granzyme B* ($P = .0121$), *TNF-α* ($P = .0022$), and *IFN-γ* ($P = .0003$) mRNA levels. There was no significant difference in perforin between these groups. The combined treatment significantly decreased *IL-6* mRNA levels ($P = .0324$) (Figure 7F,J). Taken together, these results show that the combined treatment of BET protein inhibition and anti-PD-L1 Ab effectively suppresses the progression of HCC by increasing the CD8 T cell ratio in NPCs and enhancing the activation and cytotoxic capabilities of CD8 T cells.

Finally, we developed a model to illustrate the tumor-suppressing effects of BET protein inhibition and/or PD-L1 blockade (Figure 8).

4 | DISCUSSION

Accumulating evidence suggests that cancer cell-intrinsic features shape the tumor immune landscape.[28,29] However, the tissue surrounding the microenvironment that regulates tumor immunity and sensitivity to immunotherapy remains uncertain.[30,31] This study identified a previously unknown mechanism underlying an effective therapeutic strategy of BET protein inhibition combined with an immune checkpoint Ab. Our results indicate that PD-L1 is regulated posttranscriptionally by Rab8A, which is enhanced by JQ1, and this axis serves as a key player in the regulation of HCC progression. Importantly, this combined therapeutic strategy enhances the activation and cytotoxicity of CD8 T cells to suppress the progression of HCC in vivo.

Previous studies suggest that BET protein inhibitors could be a potential choice for HCC therapy.[11,12,32] In our study, we confirmed the result that JQ1 can suppress the proliferation, migration, and invasion of HCC cells in vitro, which is consistent with the results of previous studies. However, the in vivo experiment results showed that JQ1 did not effectively inhibit HCC progression in the primary HCC mouse model, which differs from the results reported by other studies. In the transgenic HCC mouse model, our results indicated that JQ1 treatment had a weak therapeutic effect on HCC, including decreasing the maximum tumor diameter, suppressing cell proliferation, and increasing the overall survival of the mice; however, the general therapeutic effect on HCC progression was not significant. We consider that the reason for this phenomenon is related to the microenvironment and heterogeneity of HCC and the differences in the HCC mouse models used in studies, which prompted us to explore a more effective therapeutic strategy for HCC.

Immunotherapy by blocking inhibitory pathways in T lymphocytes, such as the PD-L1/PD-1 axis, has been widely studied in various solid tumors.[14,16,33,34] Immune checkpoint inhibitors have already been used in numerous clinical trials for HCC worldwide, and the outcomes are dissatisfactory. One of most serious concerns is the low or no response of HCC due to the unique immunotolerant microenvironment of the liver. Our work also did not show an antitumor effect of anti-PD-L1 Ab alone in vivo. In this study, we revealed that BET protein inhibition influences PD-L1 expression on the plasma membrane, regulated by Rab8A.

Numerous members of the Rab-GTPase family of proteins participate in assisting transmembrane proteins to package into vesicles and transport among plasma membrane and organelles. Among them, Rab8A plays irreplaceable roles in multiple biological processes, including membrane trafficking, cellular morphology, cell movement, cell polarity, neural differentiation, and ciliogenesis.[35] Furthermore, Rab8A regulates fusion between vesicles and the cell membrane.[36] We identified for the first time that the BET protein inhibitor JQ1 enhanced the expression level of Rab8A. This work also shows that Rab8A plays an important role in the distribution and expression of PD-L1 in cells. However, we did not undertake more in-depth research on this aspect, and the specific mechanism is still unclear. This effector mechanism requires further investigation for additional signaling pathways.

A number of studies have focused on the relationship between BET protein inhibitors and PD-L1 expression in various cancer models. Inhibition of BET proteins suppresses PD-L1 expression and limits its tumor progression in ovarian cancer in mice.[37] JQ1 results in a reduction of PD-L1 protein expression in neuroblastoma xenograft mouse model.[38] However, we found that JQ1 treatment did not change the total protein level of PD-L1 in HCC cells in vivo or in vitro. We consider that the reason that BET protein inhibition differentially regulated PD-L1 expression in different cancer models is due to the unique features of HCC. The underlying mechanisms causing this disparity in different cancer models are currently unknown and require further investigation.

The combined treatment of JQ1 and anti-PD-L1 Ab showed robust suppression of tumor progression in the transgenic HCC mouse model. Previous studies have suggested that BET protein inhibition cooperates with the PD-1/PD-L1 axis to mediate tumor progression in various mouse models, but the mechanism remains unclear. JQ1 decreases BRD4 occupancy at the PD-1 locus, causing transcriptional pausing and rapid loss of PD-1 mRNA production. Targeting the PD-1/PD-L1 axis by combining anti-PD-1 Abs and JQ1 causes synergistic responses in mice bearing Myc-driven lymphomas.[39] Combining BET protein inhibition with a PD-1 Ab offers a promising therapeutic approach for lung adenocarcinoma by reducing the numbers of tumor-infiltrating regulatory T cells and activating tumor-infiltrating T cells.[40] Our results suggested that BET protein inhibitor increased the expression level of PD-L1 on the plasma membrane, and induced the antitumor effect of the anti-PD-L1 Ab, suggesting

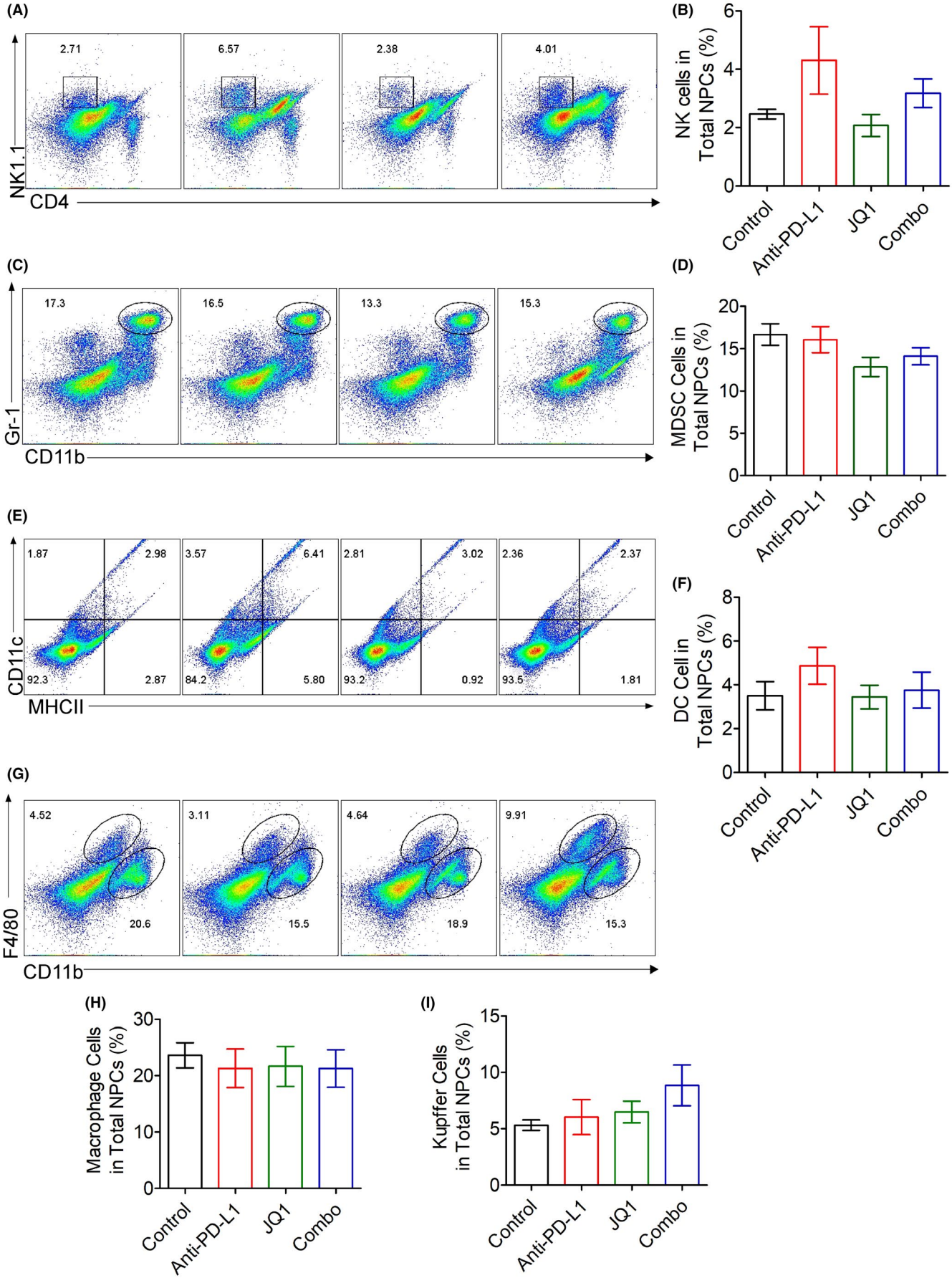
(A)
2.71
6.57
2.38
4.01
NK1.1
CD4
(B)
NK cells in Total NPCs (%)
Control
Anti-PD-L1
JQ1
Combo
(C)
17.3
16.5
13.3
15.3
Gr-1
CD11b
(D)
MDSC Cells in Total NPCs (%)
(E)
1.87
2.98
92.3
2.87
3.57
6.41
84.2
5.80
2.81
3.02
93.2
0.92
2.36
2.37
93.5
1.81
CD11c
MHCII
(F)
DC Cell in Total NPCs (%)
(G)
4.52
20.6
3.11
15.5
4.64
18.9
9.91
15.3
F4/80
CD11b
(H)
Macrophage Cells in Total NPCs (%)
(I)
Kupffer Cells in Total NPCs (%)

FIGURE 6 Inhibition of bromo- and extraterminal domain (BET) proteins combined with anti-programmed cell death-ligand 1 (PD-L1) Abs cannot affect the innate immune cell subsets in the liver. A, B, Representative flow cytometry dot plots and the percentages of natural killer (NK) cells in the total nonparenchymal cell (NPC) population. C, D, Representative flow cytometry dot plots and the percentages of myeloid-derived suppressor cells (MDSCs) in the total NPC population. E, F, Representative flow cytometry dot plots and the percentages of dendritic cells (DCs) in the total NPC population. G-I, Representative flow cytometry dot plots and the percentages of Kupffer cells and macrophages in the total NPC population. Data are shown as mean ± SEM

that PD-L1 expression is required for the antitumor effect of PD-1/PD-L1 blockade.

Numerous studies have reported that blocking the PD-L1/PD-1 axis triggers the activity of $CD8^+$ T cells, leading to an antitumor effect. Overexpression of tumor PD-L1 impairs IFN-γ secretion by $CD8^+$ CTLs.[41] Blocking the PD-1/PD-L1 axis enhances the activation of CD8 T cells in mediating antitumor immunity in HCC.[22] Our data also indicated that this combination treatment induced a tumor-inhibitory effect by enhancing the activation and cytotoxicity of CD8 T cells. These results indicate a critical role of cytotoxic CD8 T cells in mediating the antitumor immunity of HCC.

In summary, our findings reveal a key mechanism of BET protein inhibition that mediates PD-L1 expression on the plasma membrane by affecting the expression of Rab8A. Additionally, we identified an efficient combination therapy strategy for HCC therapy. Further studies focusing on the effect of BET protein inhibition and immune checkpoint blockade combination therapy on HCC in the clinical setting and the underlying mechanism of tumor biology are therefore needed.

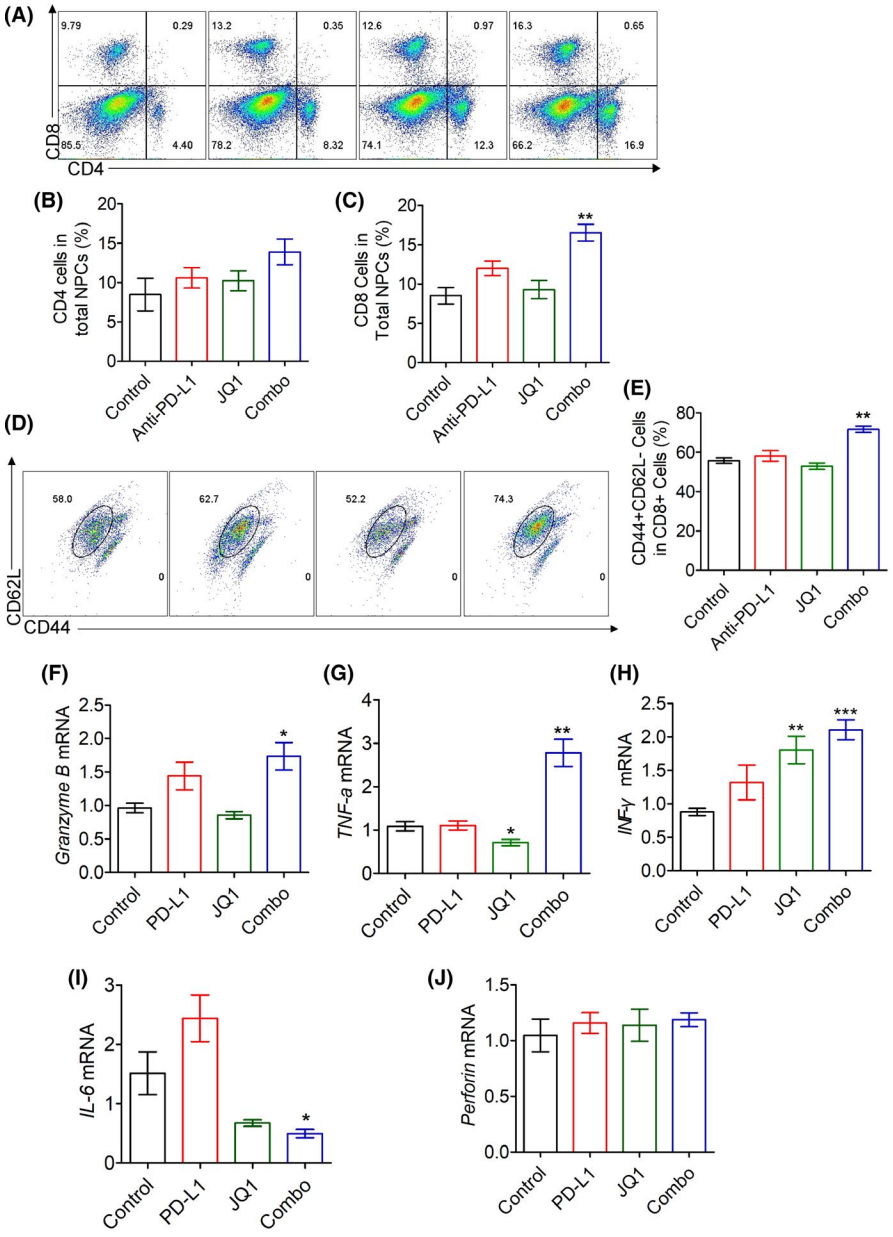

FIGURE 7 Sensitization of programmed cell death-ligand 1 (PD-L1) blockade by bromo- and extraterminal domain (BET) protein inhibition boosts antitumor immunity in the liver. A-C, Representative flow cytometry dot plots and the percentages of CD4 T cells and CD8 T cells in the total nonparenchymal cell (NPC) population. D, E, CD8 T cells were gated, and further gating was carried out for cell activation: $CD44^+CD62L^-$. F-J, Fold change in *granzyme B*, *TNF-α*, *IFN-γ*, *IL-6*, and *perforin* mRNA expression levels in CD8 T cells isolated from NPCs. Data are shown as mean ± SEM (*$P < .05$, **$P < .01$, ***$P < .001$)

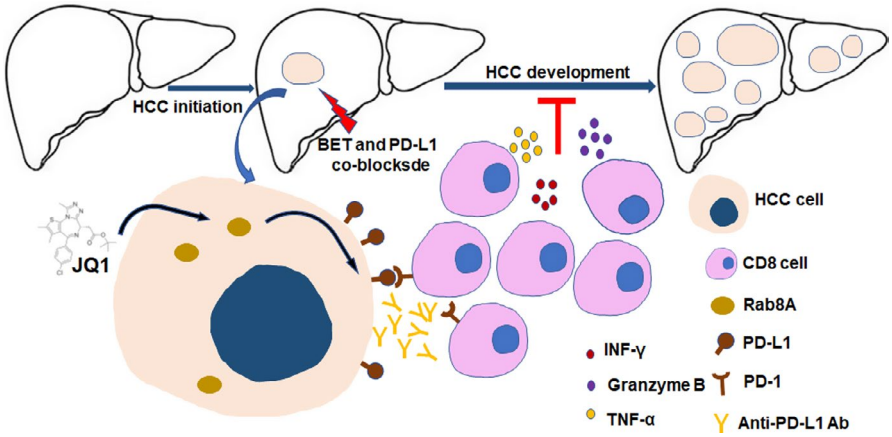

FIGURE 8 Model for the tumor-suppressing effects of bromo- and extraterminal domain (BET) protein inhibition combined with programmed cell death-ligand 1 (PD-L1) blockade. Treatment with JQ1 enhanced the expression of Rab8A, subsequently inducing PD-L1 expression on the plasma membrane of hepatocellular carcinoma (HCC), which sensitized the liver response to anti-PD-L1 blockade. Thus, a combined treatment of JQ1 and anti-PD-L1 Ab was an effective combination immunotherapy for HCC. IFN-γ, interferon-γ; PD-1, programmed cell death-1; TNF-α, tumor necrosis factor-α

ACKNOWLEDGMENTS

The project was supported by the National Science Foundation for Outstanding Young Scholars of China (No. 81522006), the Fundamental Research Funds for the Central Universities (2015XZZX004-21), the National Natural Science Foundation of China (No. 81470527, No. 81870306), Zhejiang Provincial 151 Talent Project, and Zhejiang Provincial Outstanding Youth Foundation (No. LR13H020001).

ETHICAL CONSIDERATIONS

All animal work performed in this study was approved by Institutional Animal Care and Ethics Use Committee of Zhejiang University. Animals were maintained in pathogen-free conditions and cared for according to the International Association for Assessment and Accreditation of Laboratory Animal Care policies and certification.

DISCLOSURE

The authors declare no potential conflicts of interest.

ORCID

Weilin Wang https://orcid.org/0000-0001-9432-2649
Weihua Gong https://orcid.org/0000-0002-3221-4316

REFERENCE

1. Llovet JM, Zucman-Rossi J, Pikarsky E, et al. Hepatocellular carcinoma. *Nat Rev Dis Primers*. 2016;2:16018.
2. Global Burden of Disease Cancer C, Fitzmaurice C, Allen C, et al. Global, regional, and national cancer incidence, mortality, years of life lost, years lived with disability, and disability-adjusted life-years for 32 cancer Groups, 1990 to 2015: a systematic analysis for the global burden of disease study. *JAMA Oncol*. 2017;3(4):524-548.
3. Llovet JM, Ricci S, Mazzaferro V, et al. Sorafenib in advanced hepatocellular carcinoma. *N Engl J Med*. 2008;359(4):378-390.
4. Llovet JM, Montal R, Sia D, Finn RS. Molecular therapies and precision medicine for hepatocellular carcinoma. *Nat Rev Clin Oncol*. 2018;15(10):599-616.
5. Bruix J, Qin S, Merle P, et al. Regorafenib for patients with hepatocellular carcinoma who progressed on sorafenib treatment (RESORCE): a randomised, double-blind, placebo-controlled, phase 3 trial. *Lancet*. 2017;389(10064):56-66.
6. Kudo M, Finn RS, Qin S, et al. Lenvatinib versus sorafenib in first-line treatment of patients with unresectable hepatocellular carcinoma: a randomised phase 3 non-inferiority trial. *Lancet*. 2018;391(10126):1163-1173.
7. Abou-Alfa GK, Meyer T, Cheng AL, et al. Cabozantinib in patients with advanced and progressing hepatocellular carcinoma. *N Engl J Med*. 2018;379(1):54-63.
8. Alghamdi S, Khan I, Beeravolu N, et al. BET protein inhibitor JQ1 inhibits growth and modulates WNT signaling in mesenchymal stem cells. *Stem Cell Res Ther*. 2016;7:22.
9. Gilan O, Rioja I, Knezevic K, et al. Selective targeting of BD1 and BD2 of the BET proteins in cancer and immunoinflammation. *Science*. 2020;368(6489):387-394.
10. Zhang L, Tong Y, Zhang X, Pan M, Chen S. Arsenic sulfide combined with JQ1, chemotherapy agents, or celecoxib inhibit gastric and colon cancer cell growth. *Drug Des Devel Ther*. 2015;9:5851-5862.
11. Wang YH, Sui XM, Sui YN, et al. BRD4 induces cell migration and invasion in HCC cells through MMP-2 and MMP-9 activation mediated by the Sonic hedgehog signaling pathway. *Oncol Lett*. 2015;10(4):2227-2232.
12. Zhang P, Dong Z, Cai J, et al. BRD4 promotes tumor growth and epithelial-mesenchymal transition in hepatocellular carcinoma. *Int J Immunopathol Pharmacol*. 2015;28(1):36-44.
13. Li GQ, Guo WZ, Zhang Y, et al. Suppression of BRD4 inhibits human hepatocellular carcinoma by repressing MYC and enhancing BIM expression. *Oncotarget*. 2016;7(3):2462-2474.
14. Chen DS, Mellman I. Elements of cancer immunity and the cancer-immune set point. *Nature*. 2017;541(7637):321-330.
15. Jiang X, Xu J, Liu M, et al. Adoptive CD8(+) T cell therapy against cancer: challenges and opportunities. *Cancer Lett*. 2019;462:23-32.
16. Topalian SL, Drake CG, Pardoll DM. Immune checkpoint blockade: a common denominator approach to cancer therapy. *Cancer Cell*. 2015;27(4):450-461.
17. Akinleye A, Rasool Z. Immune checkpoint inhibitors of PD-L1 as cancer therapeutics. *J Hematol Oncol*. 2019;12(1):92.

18. Hui E, Cheung J, Zhu J, et al. T cell costimulatory receptor CD28 is a primary target for PD-1-mediated inhibition. *Science*. 2017;355(6332):1428-1433.
19. El-Khoueiry AB, Sangro B, Yau T, et al. Nivolumab in patients with advanced hepatocellular carcinoma (CheckMate 040): an open-label, non-comparative, phase 1/2 dose escalation and expansion trial. *Lancet*. 2017;389(10088):2492-2502.
20. Zhu AX, Finn RS, Edeline J, et al. Pembrolizumab in patients with advanced hepatocellular carcinoma previously treated with sorafenib (KEYNOTE-224): a non-randomised, open-label phase 2 trial. *Lancet Oncol*. 2018;19(7):940-952.
21. Liu Z, Lin Y, Zhang J, et al. Molecular targeted and immune checkpoint therapy for advanced hepatocellular carcinoma. *J Exp Clin Cancer Res*. 2019;38(1):447.
22. Wen L, Xin B, Wu P, et al. An efficient combination immunotherapy for primary liver cancer by harmonized activation of innate and adaptive immunity in mice. *Hepatology*. 2019;69(6):2518-2532.
23. Cha JH, Chan LC, Li CW, Hsu JL, Hung MC. Mechanisms controlling PD-L1 expression in cancer. *Mol Cell*. 2019;76(3):359-370.
24. Li G, Marlin MC. Rab family of GTPases. *Methods Mol Biol*. 2015;1298:1-15.
25. Diekmann Y, Seixas E, Gouw M, Tavares-Cadete F, Seabra MC, Pereira-Leal JB. Thousands of rab GTPases for the cell biologist. *PLoS Comput Biol*. 2011;7(10):e1002217.
26. Langemeyer L, Frohlich F, Ungermann C. Rab GTPase function in endosome and lysosome biogenesis. *Trends Cell Biol*. 2018;28(11):957-970.
27. Reddy JM, Raut NGR, Seifert JL, Hynds DL. Regulation of small GTPase prenylation in the nervous system. *Mol Neurobiol*. 2020;57(5):2220-2231.
28. Syn NL, Teng MWL, Mok TSK, Soo RA. De-novo and acquired resistance to immune checkpoint targeting. *Lancet Oncol*. 2017;18(12):e731-e741.
29. Wellenstein MD, de Visser KE. Cancer-cell-intrinsic mechanisms shaping the tumor immune landscape. *Immunity*. 2018;48(3):399-416.
30. Ribas A, Wolchok JD. Cancer immunotherapy using checkpoint blockade. *Science*. 2018;359(6382):1350-1355.
31. Fu Y, Liu S, Zeng S, Shen H. From bench to bed: the tumor immune microenvironment and current immunotherapeutic strategies for hepatocellular carcinoma. *J Exp Clin Cancer Res*. 2019;38(1):396.
32. Yin Y, Sun M, Zhan X, et al. EGFR signaling confers resistance to BET inhibition in hepatocellular carcinoma through stabilizing oncogenic MYC. *J Exp Clin Cancer Res*. 2019;38(1):83.
33. Chen L, Han X. Anti-PD-1/PD-L1 therapy of human cancer: past, present, and future. *J Clin Invest*. 2015;125(9):3384-3391.
34. Whiteside TL, Demaria S, Rodriguez-Ruiz ME, Zarour HM, Melero I. Emerging opportunities and challenges in cancer immunotherapy. *Clin Cancer Res*. 2016;22(8):1845-1855.
35. Peranen J. Rab8 GTPase as a regulator of cell shape. *Cytoskeleton (Hoboken)*. 2011;68(10):527-539.
36. Bond LM, Peden AA, Kendrick-Jones J, Sellers JR, Buss F. Myosin VI and its binding partner optineurin are involved in secretory vesicle fusion at the plasma membrane. *Mol Biol Cell*. 2011;22(1):54-65.
37. Zhu H, Bengsch F, Svoronos N, et al. BET bromodomain inhibition promotes anti-tumor immunity by suppressing PD-L1 expression. *Cell Rep*. 2016;16(11):2829-2837.
38. Melaiu O, Mina M, Chierici M, et al. PD-L1 is a therapeutic target of the bromodomain inhibitor JQ1 and combined with HLA class I, a promising prognostic biomarker in neuroblastoma. *Clin Cancer Res*. 2017;23(15):4462-4472.
39. Hogg SJ, Vervoort SJ, Deswal S, et al. BET-bromodomain inhibitors engage the host immune system and regulate expression of the immune checkpoint ligand PD-L1. *Cell Rep*. 2017;18(9):2162-2174.
40. Adeegbe DO, Liu S, Hattersley MM, et al. BET bromodomain inhibition cooperates with PD-1 blockade to facilitate antitumor response in Kras-Mutant non-small cell lung cancer. *Cancer Immunol Res*. 2018;6(10):1234-1245.
41. Huang CY, Wang Y, Luo GY, et al. Relationship between PD-L1 expression and CD8+ T-cell immune responses in hepatocellular carcinoma. *J Immunother*. 2017;40(9):323-333.

SUPPORTING INFORMATION

Additional supporting information may be found online in the Supporting Information section.

How to cite this article: Liu C, Miao X, Wang Y, et al. Bromo- and extraterminal domain protein inhibition improves immunotherapy efficacy in hepatocellular carcinoma. *Cancer Sci*. 2020;111:3503–3515. https://doi.org/10.1111/cas.14588